86.2 (8)°, C(21)–Mn(2)–C(23) = 94.5 (7)°, and C(22)–Mn(2)–C(23) = 98.0 (8)°. The (η^5-dienyl)Mn(CO)$_3$ moiety has close to C_s symmetry; the carbonyl group C(23)–O(23) lies almost between (and below) the ends of the η^5-dienyl system and the reduced OC–Mn–CO angle is between the other two carbonyl groups. A similar situation occurs both in (azulene)Mn$_2$(CO)$_6$[13] and in (η^5-cyclohexadienyl)tricarbonylmanganese.[14]

Finally we note that Mn–CO and C–O distances are normal and that the Mn–C–O systems are each close to linear.

Acknowledgment. We thank Professor R. B. King for providing the sample. This work has been generously supported by the National Foundation (Grant No. CHE77-04981, to M.R.C.).

Registry No. $(C_{14}H_8Me_2)Mn_2(CO)_6$, 67505-76-4.

Supplementary Material Available: A listing of structure factor amplitudes (5 pages). Ordering information is given on any current masthead page.

References and Notes

(1) M. R. Churchill, *Prog. Inorg. Chem.*, **11**, 53–98 (1970).
(2) M. R. Churchill, R. A. Lashewycz, and F. J. Rotella, *Inorg. Chem.*, **16**, 265 (1977); see also ref 1–9 contained therein.
(3) M. R. Churchill and J. Wormald, *Inorg. Chem.*, **9**, 2239 (1970).
(4) M. R. Churchill and J. Wormald, *Inorg. Chem.*, **8**, 1970 (1969).
(5) M. R. Churchill and B. G. DeBoer, *Inorg. Chem.*, **12**, 525 (1973).
(6) M. R. Churchill and K. G. Lin, *Inorg. Chem.*, **12**, 2274 (1973).
(7) K. Hafner and J. Schneider, *Justus Liebigs Ann. Chem.*, **624**, 37 (1959).
(8) (a) M. R. Churchill, S. A. Julis, R. B. King, and C. A. Harmon, *J. Organomet. Chem.*, **142**, C52 (1977); (b) M. R. Churchill and S. A. Julis, *Inorg. Chem.*, **17**, 1453 (1978).
(9) M. R. Churchill, F. J. Hollander, and J. P. Hutchinson, *Inorg. Chem.*, **16**, 2655 (1977).
(10) "Syntex XTL Operations Manual", 2nd ed, Syntex Analytical Instruments, Cupertino, Calif., 1976.
(11) "International Tables for X-Ray Crystallography", Vol. IV, Kynoch Press, Birmingham, England, 1974: (a) pp 99–101; (b) pp 149–150.
(12) M. R. Churchill, *Inorg. Chem.*, **12**, 1213 (1973).
(13) M. R. Churchill and P. H. Bird, *Inorg. Chem.*, **7**, 1793 (1968).
(14) M. R. Churchill and F. R. Scholer, *Inorg. Chem.*, **8**, 1950 (1969).

Notes

Contribution from the Department of Chemistry,
The University of North Carolina,
Chapel Hill, North Carolina 27514

Intervalence Transfer in the Pyrimidine-Bridged Dimer $[(bpy)_2ClRu(pym)RuCl(bpy)_2]^{3+}$

Michael J. Powers and Thomas J. Meyer*

Received October 24, 1977

In earlier work[1-5] we have shown that in mixed-valence complexes of the type $[(bpy)_2ClRu(L)RuCl(bpy)_2]^{3+}$ (bpy is 2,2′-bipyridine, L = pyrazine (pyr), 4,4′-bipyridine (4,4′-bpy), *trans*-1,2-bis(4-pyridyl)ethylene (BPE)) there are localized Ru(II) and Ru(III) sites, at least on the vibrational time scale. The optical spectra of these complexes include low-energy absorption bands which have been assigned to intervalence transfer (IT)[6] transitions (eq 1). In an IT transition,

$$[\mathrm{Ru(II)\text{-}Ru(III)}] \xrightarrow{h\nu} [\mathrm{Ru(III)\text{-}Ru(II)}]^* \tag{1}$$

long-range optical electron transfer occurs between localized redox sites.[6] IT transitions have been treated theoretically by Hush[6] and the Ru(bpy) complexes have been used experimentally to demonstrate the predicted dependence of E_{op} (the energy of the IT band at $\lambda_{\max}$) on solvent properties[2,4,5] and of E_{op} on the distance between redox sites.[4] The same experimental results using the Ru(bpy) complexes have also been valuable in pointing out the close relationship between inner-sphere electron transfer between redox sites where the extent of delocalization is slight and related outer-sphere electron-transfer processes.[2,4]

Since the dimeric Ru(bpy) systems have well-defined mixed-valence properties and a well-developed synthetic chemistry, they can be modified chemically in ways which allow for the study of the effects of relatively subtle molecular changes on mixed-valence properties. One of the most important variations is in the nature of the bridging ligand.[7] In the dimers $[(bpy)_2ClRu(L)RuCl(bpy)_2]^{3+}$, the most likely orbital pathways for Ru(II)–Ru(III) interaction are through the mixing of $d\pi$(Ru(II)) with π^*(L) orbitals which "carries" the excess electron across the bridging ligand to Ru(III) or the mixing of $d\pi$(Ru(III)) and filled π(L) levels which leads to electron hole delocalization. If this view is correct, the electronic structure of the bridging ligand should play an important role in determining the extent of electron delocalization from Ru(II) to Ru(III) in the ground state.

We have prepared the dimeric complex $[(bpy)_2ClRu(pym)RuCl(bpy)_2]^{2+}$ where the bridging ligand is pyrimidine (pym) and have generated the 3+, mixed-valence ion in solution. The point of interest was the expected appearance of an IT band for the mixed-valence ion and then a comparison of its properties with the IT band for the pyrazine (pyr)-bridged dimer $[(bpy)_2ClRu(pyr)RuCl(bpy)_2]^{3+}$. The Ru–Ru separation is shorter in the pyrimidine-bridged complex, but earlier work using pyrimidine as a ligand had suggested that the transmission of electronic effects between groups bound to meta-nitrogen atoms through the π^* system of the diazine ring can be relatively ineffective.[8,9]

Experimental Section

Measurements. Ultraviolet–visible spectra were obtained using Cary Model 14, Cary Model 17, and Bausch and Lomb Spectronic 210 spectrophotometers at room temperature. Near-infrared spectra were recorded on a Cary Model 17 spectrophotometer. Electrochemical measurements were made vs. the saturated sodium chloride calomel electrode (SSCE) at 25 ± 2 °C using Pt bead electrodes and are uncorrected for junction potential effects. The measurements were made using a PAR Model 173 potentiostat for potential control with a PAR Model 175 universal programmer as a sweep generator for voltammetric experiments.

Materials. Tetra-*n*-butylammonium hexafluorophosphate (TBAH) was prepared by standard techniques,[1,10] recrystallized twice from hot ethanol–water mixtures and vacuum dried at 70 °C for 10 h. Acetonitrile (MCB Spectrograde) was dried over Davison 4-Å molecular sieves for electrochemical measurements and used without drying for spectral measurements. Pyrimidine was purchased commercially and used without further purification. Elemental analyses were carried out by Integral Microanalytical Inc., Raleigh, N.C.

Preparations. $[(bpy)_2ClRu(pym)RuCl(bpy)_2](PF_6)_2\cdot H_2O$ (bpy Is 2,2′-Bipyridine and pym Is Pyrimidine). This complex was prepared using methods described earlier[1-3,11] for similar bis(bipyridine)ruthenium dimers. $[(bpy)_2ClRu(pym)](PF_6)$ was prepared from $[(bpy)_2ClRu(NO)](PF_6)_2$ (0.483 g, 0.628 mmol) by dissolving the nitrosyl complex in ~30 mL of acetone and adding, dropwise, KN_3 (0.051 g, 0.629 mmol) dissolved in a minimum (~5 mL) of methanol. After ~15 min of stirring in the dark, excess pyrimidine was added to the burgundy-colored solution and it was heated at reflux for 20 h. The acetone solution was then filtered through a glass frit to remove insoluble KPF_6 and added dropwise to ~175 mL of stirred anhydrous ether. The PF_6^- salt, which precipitated immediately, was collected by suction filtration and reprecipitated by dissolving it in a minimum amount of acetone and adding this solution to ether.

The dimeric complex was prepared by dissolving $[(bpy)_2ClRu(NO)](PF_6)_2$ (0.581 g, 0.756 mmol) in acetone (~30 mL) and adding, dropwise, KN_3 (0.062 g, 0.756 mmol) dissolved in a minimum (~5 mL) of methanol. After about 15 min of stirring in the dark, $[(bpy)_2ClRu(pym)](PF_6)$ (0.510 g, 0.756 mmol) dissolved in ~20 mL of acetone was added and the solution heated at reflux for 20 h. After 20 h, the volume of acetone was reduced to about 15 mL and this was filtered through a glass frit into anhydrous ether. The precipitate was collected by suction filtration and reprecipitated by dissolving it in a minimum amount of acetone and adding it to ether.

The dimer was purified by dissolving the complex in CH_2Cl_2, placing it on the top of an alumina column, and eluting with a 2% solution of methanol in CH_2Cl_2. The yield after column chromatography was 70%. Anal. Calcd for $[(bpy)_2ClRu(pym)RuCl(bpy)_2](PF_6)_2 \cdot H_2O$: C, 41.10; H, 2.98; N, 10.89. Found: C, 41.13; H, 2.51; N, 10.60.

$[(bpy)_2ClRu(pym)RuCl(bpy)_2]^{3+/4+}$. The oxidized complexes were not isolated but were generated in solution either by electrochemical oxidation or by chemical oxidation using $(NH_4)_2Ce(NO_3)_6$. The fact that we have not isolated salts of the oxidized ions comes from their long term instability in solution.[13]

Results

The preparations of the ligand-bridged dimers $[(bpy)_2ClRu(L)RuCl(bpy)_2]^{2+}$ where L equals[11]

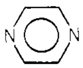

pyr

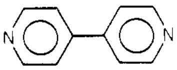

4,4′-bpy

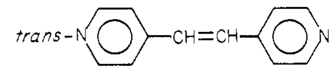

BPE

or pyrimidine all involve solvent displacement reactions to form the bridge between metal centers. For the pyrimidine case, a noticeably longer reflux time was required for the dimer to appear as a reaction product. Molecular models indicate that the complex can be prepared but that the longer reaction times may arise because of steric constraints. Rotation about the ruthenium–pyrimidine bonds is severely restricted because of the bulkiness of the 2,2′-bipyridine ligands and the Ru–Cl groups which occupy the position cis to the bridging ligand are held in closely adjacent, relatively fixed positions.

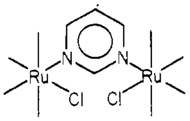

The 2+ dimer is thermally stable in acetonitrile but is light sensitive. Exposure of an acetonitrile solution to fluorescent room lighting for 10 min causes a 20% bleaching of the 481-nm peak in its absorption spectrum (see spectrum below).

In Table I are summarized spectral data and $E_{1/2}$ values obtained from cyclic voltammetric experiments. The optical spectra for both the monomeric and dimeric complexes are very similar to the spectra reported earlier[2,3] for related complexes like $[Ru(bpy)_2(pyr)Cl]^+$ and $[(bpy)_2ClRu(pyr)RuCl(bpy)_2]^{2+}$. They include the usual $d\pi(Ru)$ to π^* (ligand) charge-transfer (MLCT) absorption bands in the visible and internal ligand $\pi \rightarrow \pi^*$ (bpy) absorption bands in the ultraviolet.[12] An interesting point to note is that the lowest energy CT band at λ_{max} 481 nm in the pyrimidine-bridged 2+ dimer is shifted to higher energy compared to the monomer $[Ru(bpy)_2(pym)Cl]^+$. This is in contrast to the related dimers $[(bpy)_2ClRu(L)RuCl(bpy)_2]^{2+}$ where, compared to the appropriate monomers, there is a red shift in the lowest CT band energy for L = 4,4′-bpy or BPE. For L = pyr a new and distinct low-energy absorption band appears which is assignable to a $\pi^*(pyr) \leftarrow d\pi(Ru)$ transition rather than to $\pi^*(bpy) \leftarrow d\pi(Ru)$.[2,3,11]

The electrochemical results are very similar to those found earlier[2,3,5] for the pyrazine-bridged dimer in that there are two closely spaced, reversible oxidation waves. $E_{1/2}$ values were calculated for the two waves from the average of the anodic and cathodic peak potentials ($E_{1/2} = (E_{p,a} + E_{p,c})/2$). Except for the usually small correction for differences in diffusion coefficients, the values are formal reduction potentials for the couples in eq 2 and 3. For the pyrazine-bridged dimer, $E_{1/2}(1) = 0.89$ V and $E_{1/2}(2) = 1.01$ V under the same experimental conditions.

Table I. Spectral and Electrochemical Data for Ruthenium–Pyrimidine Complexes in Acetonitrile at Room Temperature

complex	λ_{max},[a] nm	$10^{-3}\epsilon$[b]	$E_{1/2}$, V (ΔE_p, mV)[c]
$[(bpy)_2ClRu(pym)]^+$	490	8.94	0.84 (70)
	455 sh		
	360	9.58	
	293	52.8	
	285 sh		
	255 sh		
	240	21.1	
$[(bpy)_2ClRu(pymH)]^{2+}$ [d]			0.97 (65)
$[(bpy)_2ClRu(pym)]^{2+}$	423	2.59	
	350 sh		
	312	29.9	
	300	2.80	
	246	28.3	
$[(bpy)_2ClRu(pym)RuCl(bpy)_2]^{2+}$	481	20.2	0.87 (60)
	~450 sh		0.99 (60)
	~390 sh		
	349	15.2	
	293	106.0	
	285 sh		
	255 sh		
	242	49.5	
$[(bpy)_2ClRu(pym)RuCl(bpy)_2]^{3+}$	482	13.6	
	450 sh		
	343	12.6	
	313 sh		
	293	70.3	
	243	34.4	
$[(bpy)_2ClRu(pym)RuCl(bpy)_2]^{4+}$	425	4.93 sh	
	345	9.13	
	313	47.2	
	298	47.2	
	247	46.3	

[a] ±2 nm. [b] Estimated error in values is ±5%. [c] $E_{1/2}$ values are in 0.1 M $[N(n\text{-}C_4H_9)_4](PF_6)$(TBAH)–$CH_3CN$ vs. the saturated sodium chloride calomel electrode (SSCE). ΔE_p values which are the differences between anodic and cathodic peak potentials from cyclic voltammetry are sweep rate independent from 200 mV/s to 1 V/s. [d] Generated by adding $HClO_4$ to $[(bpy)_2ClRu(pym)]^+$ in 0.1 M TBAH/CH_3CN.

$$[(bpy)_2ClRu(pym)RuCl(bpy)_2]^{4+} + e^- \rightarrow [(bpy)_2ClRu(pym)RuCl(bpy)_2]^{3+} \quad E_{1/2}(2) = 0.99 \text{ V} \tag{2}$$

$$[(bpy)_2ClRu(pym)RuCl(bpy)_2]^{3+} + e^- \rightarrow [(bpy)_2ClRu(pym)RuCl(bpy)_2]^{2+} \quad E_{1/2}(1) = 0.87 \text{ V} \tag{3}$$

Solutions of the 3+, mixed-valence ion $[(bpy)_2ClRu(pym)RuCl(bpy)_2]^{3+}$ or of the 4+, Ru(III)–Ru(III) ion $[(bpy)_2ClRu(pym)RuCl(bpy)_2]^{4+}$ were generated either by controlled-potential electrolysis to $n = 1$ or $n = 2$, respectively, or by chemical oxidation using Ce(IV).[13] A spectrophotometric titration with Ce(IV) showed that upon oxidation a steady decrease in absorbance occurs both at λ_{max} 481 nm and at the higher energy shoulder at ~340 nm. There are no new absorption bands, and initially no band shifts in the visible or near-ultraviolet region. Complete oxidation results in the loss of the visible band at 481 nm leaving a shoulder characteristic of Ru(III) complexes[1,3] at λ_{max} 425 nm.

Upon oxidation of $[(bpy)_2ClRu(pym)RuCl(bpy)_2]^{2+}$ to the 3+ mixed-valence ion, a weak absorption band appears in the near-infrared region.[14] From the potential difference between $E_{1/2}(1)$ and $E_{1/2}(2)$ (120 mV), K for the conproportionation equilibrium (eq 4) is 107. Using the K value to correct for

$$[(bpy)_2ClRu(pym)RuCl(bpy)_2]^{2+} + [(bpy)_2ClRu(pym)RuCl(bpy)_2]^{4+} \rightleftharpoons 2[(bpy)_2ClRu(pym)RuCl(bpy)_2]^{3+} \quad (4)$$

the small amounts of the 2+ and 4+ ions which are present at equilibrium allows the molar extinction coefficient for the mixed-valence ion to be calculated in the near-infrared region giving ϵ 34 ± 3 $M^{-1}\,cm^{-1}$ at 1360 ± 5 nm.[14]

The bandwidth at half-height, $\Delta\bar{\nu}_{1/2} = 0.552\ \mu m^{-1}$, for the near-infrared band was estimated by doubling the half-bandwidth at half-height on the high-energy side of $\bar{\nu}_{max}$. It was not possible to use the procedure suggested by Hush[6] because of tailing of the near-infrared band on the low-energy side into regions of background solvent absorption. The experimental bandwidth is greater than that predicted by eq

$$\bar{\nu}_{max} = (\Delta\bar{\nu}_{1/2})^2/2.31 \quad (5)$$

5 (0.412 μm^{-1}) which assumes a Gaussian band shape and is based on a single oscillator model.[6] The greater experimental bandwidth is not unexpected and the ratio $\Delta\bar{\nu}_{1/2}(obsd)/\Delta\bar{\nu}_{1/2}(calcd) = 1.34$ is in the same range as found for a series of $[(bpy)_2ClRu^{II}(L)Ru^{III}Cl(bpy)_2]^{3+}$ mixed-valence ions.[4b]

Using the experimental bandwidth and extinction coefficients at λ_{max} allows α^2 ($=3.0 \times 10^{-4}$) to be calculated using eq 6.[6] For a mixed-valence ion having localized valences, α^2

$$\alpha^2 = \frac{(4.2 \times 10^{-4})\epsilon_{max}\Delta\bar{\nu}_{1/2}}{\bar{\nu}_{max}d^2} \quad (6)$$

gives an estimate of the extent of delocalization of the optical electron in the ground state.[6] In eq 6, ϵ_{max} is the extinction coefficient at $\bar{\nu}_{max}$, and d is the internuclear separation between the Ru(II) and Ru(III) sites (6.0 Å).

Discussion

The width and position of the near-infrared band and the similarities in spectral and redox properties between the pyrazine- and pyrimidine-bridged dimers argue that there are localized Ru(II) and Ru(III) sites in $[(bpy)_2ClRu(pym)RuCl(bpy)_2]^{3+}$. The near-infrared band can then be reasonably assigned to an IT transition (eq 7) involving optical

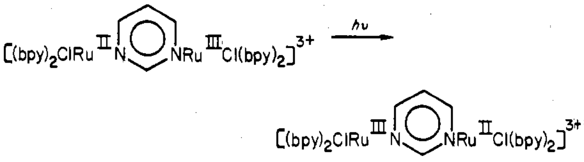

(7)

electron transfer from Ru(II) to Ru(III). The similarities in UV–visible spectra and redox properties show that the gross electronic environments at the Ru(II) and Ru(III) sites are nearly the same in the two dimers. Even though both mixed-valence dimers contain localized Ru(II) and Ru(III) sites, there are noticeable differences in the properties of their IT bands. The differences are predictable given the properties of the two bridging ligands and they point out that IT bands in localized mixed-valence ions are sensitive in a rational way to relatively subtle changes in molecular geometry and electronic structure. The differences also reinforce the view that the optical and thermal electron-transfer properties of such systems can be varied predictably by controlled synthetic modifications.

For the mixed-valence ions $[(bpy)_2ClRu(L)RuCl(bpy)_2]^{3+}$ (L = pyr, 4,4′-bpy, and BPE), a linear correlation has been found between E_{op} and $-1/d$ where d is the internuclear separation between the Ru(II) electron donor and Ru(III) acceptor sites.[4,11c] For the pyrimidine-bridged dimer, the Ru(II)–Ru(III) separation (6.0 Å) is less than for the pyrazine dimer (6.9 Å) and E_{op} is less as expected. In fact, as will be discussed in a later paper,[11c] the simple $-1/d$ dependence is not appropriate for the ions where L = pym, pyr, or 4,4′-bpy but the E_{op} data can be treated quantitatively by making a slight empirical correction. Unfortunately, the instability of the dimer precluded a study of the dependence of E_{op} on solvent.

Even though the Ru(II)–Ru(III) separation is less for the pyrimidine dimer, the oscillator strength of its IT band is significantly lower. The calculated values for α^2 are 3.0×10^{-4} and 2.6×10^{-3} for the pyrimidine- and pyrazine-bridged dimers, respectively, in acetonitrile (0.1 M in TBAH for the pyrimidine-bridged dimer). In fact, the value for α^2 is much nearer that for the BPE-bridged dimer (α^2 is between 1.5×10^{-4} and 3.0×10^{-4})[11c] where the Ru(II)–Ru(III) separation is 13.2 Å. In the Hush treatment, α^2 is a measure of the extent of delocalization of the optical electron and delocalization occurs by overlap and mixing of appropriate wave functions at the Ru(II) and Ru(III) sites. The much lower α^2 value for the pyrimidine dimer suggests that there is a considerably diminished overlap of Ru(II) and Ru(III) wave functions when the Ru sites are located at the meta compared to the para positions in the diazine ring system.

There is other experimental evidence to suggest that interactions between chemical sites through the diazine ring system vary markedly between the meta and para cases. The lowest energy MLCT band in $[(bpy)_2ClRu(pym)RuCl(bpy)_2]^{2+}$ is blue-shifted compared to the monomer $[Ru(bpy)_2(pym)Cl]^+$ and red-shifted in the other 2+ dimers $[(bpy)_2ClRu(L)RuCl(bpy)_2]^{2+}$. In the pentaammine complex $[(NH_3)_5Ru(pym)]^{2+}$ there is a decrease in basicity at the unbound N atom site compared to the free ligand and only a slight enhancement in basicity in the $\pi^*(pym) \leftarrow d\pi(Ru)$ excited state. This is in contrast to the pyrazine complex $[(NH_3)_5Ru(pyr)]^{2+}$ where there is a striking increase in basicity in both the ground and MLCT excited states.[8]

Molecular orbital (CNDO, INDO) calculations on the free ligands show that for pyrazine the lowest π^* level is at lower energy compared to pyrimidine and the atomic coefficients at the nitrogen atoms are higher for pyrazine.[15] The differences in electronic structure at the bridging ligand may account for the difference in electronic coupling between the two redox sites. For the case where L = pyrimidine, outer-sphere orbital overlap must also be taken into account. The two Ru–Cl sites are held in a near close contact geometry by the combination of the bridging ligand and restricted rotation around the Ru–pym–Ru bonds. Recent work has shown the existence of an outer-sphere IT band within the ion-pair $[Ru^{III}(NH_3)_5py,Fe^{II}(CN)_6]^-$ (λ_{max} 905 nm, ϵ 34 ± 5) which shows that outer-sphere orbital overlap between donor and acceptor sites can be sufficient to give reasonably intense outer-sphere IT bands.[16] Regardless of the origin of the orbital overlap, the energetics of optical and thermal electron transfer between the Ru(II) and Ru(III) sites are determined by the internuclear separation between sites and not by the orbital pathway involved.

The detailed nature of the orbital pathway for electron transfer affects both the frequency factor for the rate of thermal intramolecular electron transfer[4] and the oscillator strength of the IT band.[6] If nuclear tunneling through the activation barrier for thermal electron transfer is unimportant, the optical and thermal energies for intramolecular electron transfer are determined by differences in vibrational energies in the inner- and outer-coordination spheres at the two oxidation state sites. These energy differences are significantly perturbed by delocalization effects only when orbital overlap between the sites is appreciable and should be unaffected by changes in the orbital pathway involved if delocalization is slight.

Acknowledgment. Acknowledgments are made to Army Research Office, Durham, N.C., under Grant No. DAAG29-76-G-0135 and to the National Institutes of Health under Grant No. 2-R01-GM15238-10 for support of this research.

Registry No. $[(bpy)_2ClRu(pym)](PF_6)$, 66792-58-3; $[(bpy)_2ClRu(pymH)]^{2+}$, 66792-59-4; $[(bpy)_2ClRu(pym)]^{2+}$, 66792-60-7; $[(bpy)_2ClRu(pym)RuCl(bpy)_2](PF_6)_2$, 66792-62-9; $[(bpy)_2ClRu(pym)RuCl(bpy)_2]^{3+}$, 66808-68-2; $[(bpy)_2ClRu(pym)RuCl(bpy)_2]^{4+}$, 66792-63-0; $[(bpy)_2ClRu(NO)](PF_6)_2$, 58575-12-5.

References and Notes

(1) R. W. Callahan, G. M. Brown, and T. J. Meyer, *Inorg. Chem.*, **14**, 1443 (1975).

(2) R. W. Callahan and T. J. Meyer, *Chem. Phys. Lett.*, **39**, 82 (1976); R. W. Callahan, F. R. Keene, T. J. Meyer, and D. J. Salmon, *J. Am. Chem. Soc.*, **99**, 1064 (1977).

(3) R. W. Callahan, Ph.D. Thesis, The University of North Carolina, Chapel Hill, N.C., 1975.

(4) (a) M. J. Powers, D. J. Salmon, R. W. Callahan, and T. J. Meyer, *J. Am. Chem. Soc.*, **98**, 6731 (1976); (b) M. J. Powers, Ph.D. Dissertation, The University of North Carolina, 1977; (c) T. J. Meyer, *Acc. Chem. Res.*, **11**, 94 (1978).

(5) M. J. Powers, R. W. Callahan, T. J. Meyer, and D. J. Salmon, *Inorg. Chem.*, **15**, 1457 (1976).

(6) (a) N. S. Hush, *Prog. Inorg. Chem.*, **8**, 391 (1967); (b) *Electrochim. Acta*, **13**, 1005 (1968).

(7) H. Taube, *Proc. N.Y. Acad. Sci.*, in press.

(8) P. C. Ford, D. F. Rudd, R. Gaudner, and H. Taube, *J. Am. Chem. Soc.*, **90**, 1187 (1968).

(9) P. R. Taylor, B.Sc. Honors Thesis, University of Sydney, 1973; P. R. Taylor and N. S. Hush, private communication.

(10) W. Lange and E. Müller, *Chem. Ber.*, **63**, 1058 (1930).

(11) (a) S. A. Adeyemi, J. N. Braddock, G. M. Brown, J. A. Ferguson, F. J. Miller, and T. J. Meyer, *J. Am. Chem. Soc.*, **94**, 300 (1972); (b) S. A. Adeyemi, E. C. Johnson, F. J. Miller, and T. J. Meyer, *Inorg. Chem.*, **12**, 2371 (1973); (c) M. J. Powers and T. J. Meyer, submitted for publication.

(12) G. M. Bryant, J. E. Fergusson, and H. K. J. Powell, *Aust. J. Chem.*, **24**, 257 (1971).

(13) Solutions of the oxidized ions in acetonitrile are unstable over long periods and after 2 h, noticeable decomposition occurs as shown by changes in cyclic voltammograms. The decomposition chemistry, which is unusual given the high chemical stability of related Ru(III)–Ru(III) dimeric systems, is currently under investigation. Its origin may lie in the close proximity at which the pyrimidine bridging ligand holds the Ru(III) sites. Experiments involving the oxidized ions were carried out before noticeable decomposition had occurred.

(14) The same result was obtained by generating the mixed-valence ion either by electrochemical oxidation or by oxidation with Ce(IV). However, the electrochemical experiment proved more satisfactory because a precipitate (probably a Ce(III) salt) appears following chemical oxidation and the precipitate leads to experimental difficulties in the determination of extinction coefficients.

(15) E. Kober, unpublished results.

(16) J. Curtis and T. J. Meyer, *J. Am. Chem. Soc.*, in press.

Contribution from the Department of Applied Science,
Faculty of Engineering, Kyushu University,
Fukuoka 812, Japan

Exchange Interactions in Diamminecopper(II) Carbonate

Kusuo Kamase, Keiji Osaki, and Norikiyo Uryû*

Received February 24, 1978

Some years ago, Jeter et al.[1] reported the results of investigation on the antiferromagnetic properties of the complex $Cu(NH_3)_2CO_3$. As shown in Figure 1, the structure of this complex[2,3] consists of chains of copper(II) ions. The superexchange interactions are thought to be operative through the bridging carbonate ligands or through incipient bond formation between pairs of copper ions in adjacent chains. Jeter et al. have analyzed their magnetic susceptibility measurements of a powdered sample based on two models: (A) the anisotropic Ising model of infinite chains of $s = {}^1/_2$ ions assuming that the spin–spin interactions are only operative through the bridging carbonate groups and (B) the dimer model assuming that pairs of copper ions in neighboring chains interact and give rise to singlet and triplet states only.

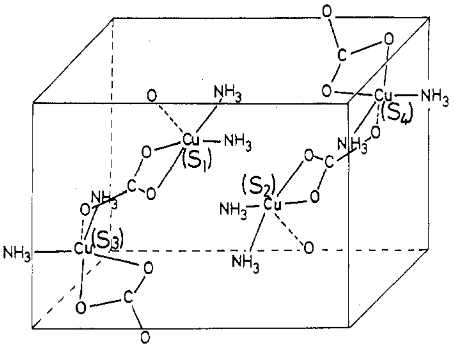

Figure 1. The structure of $Cu(NH_3)_2CO_3$. The four cluster spins $\mathbf{s}_1$, $\mathbf{s}_2$, $\mathbf{s}_3$, and $\mathbf{s}_4$ assigned to each Cu^{2+} ion are also shown.

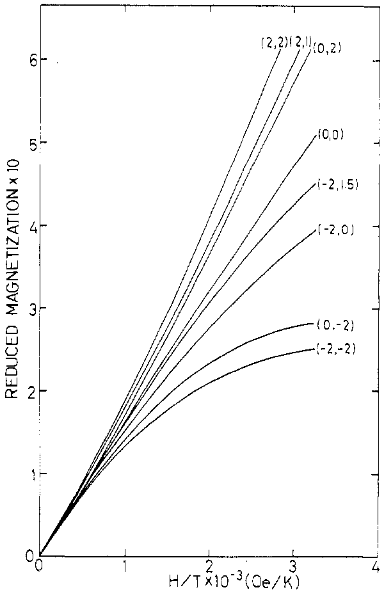

Figure 2. Variations of the reduced magnetic moment $\langle \mu \rangle$ vs. H/T calculated for various sets of values of J and J' and with $g = 2.18$. Numerical values in the parentheses denote the values of J and J' in units of cm^{-1}.

Model A turned out to be a rather poor approximation of the observation with the parameters $g = 2.20$, the Landé factor, and $J = -6.2\ cm^{-1}$, the intrachain exchange coupling constant. On the contrary, model B with the use of the modified equation by Kubo et al.[4] gave a somewhat better fit with $g = 2.19$ and $J' = -4.5\ cm^{-1}$, the interchain exchange coupling constant. By using the value of $2J'$, the energy separation between the singlet and triplet spin states, the magnetic moment in the dimer model B can be calculated by the Brillouin function for a system with $S = 1$. In an attempt to clarify the cooperative magnetic phenomenon, Jeter et al.[1] have also analyzed their magnetization data, comparing them with the above Brillouin function. However, the variation of the experimental magnetic moment $\langle \mu \rangle$ vs. H/T showed a marked deviation from the theoretical curves each calculated with $g = 2.19$ and $g = 2.0$. Thus it is evident that neither model A nor model B is sufficient to describe the magnetic behaviors of the present complex. Rather, both models should be reconciled to the